W., Jr.: Shavitt, I. *Ibid.* **1978**, *100*, 739. (g) See also: Harrison, J. F. *Acc. Chem. Res.* **1974**, *7*, 378.
(12) Kirmse, W. "Carbene Chemistry", 2nd ed.; Academic Press: New York, 1971.
(13) (a) Walsh, A. D. *Nature (London)* **1947**, *159*, 167, 712. (b) *Trans. Faraday Soc.* **1949**, *45*, 179. (c) Sugden, T. M. *Nature (London)* **1947**, *160*, 367.
(14) Salem, L.; Wright, J. S. *J. Am. Chem. Soc.* **1969**, *91*, 5947.
(15) Hoffmann, R.; Davidson, R. B. *J. Am. Chem. Soc.* **1971**, *93*, 5699.
(16) Heilbronner, E.; Bock, H. "Das HMO-Modell und Seine Anwendung", Verlag Chemie, Weinheim/Bergstr., West Germany, 1968.
(17) If **5** would adopt C_{2v} symmetry the formation of bonding between C_1 and C_3 corresponds to a symmetry-forbidden process, since a b_1 level (p AO) would cross an a_1 level (symmetric Walsh orbital).
(18) The nature of bonding in bicyclobutane has been analyzed in detail. (a) Newton, M. D.; Schulman, J. M. *J. Am. Chem. Soc.* **1974**, *96*, 6295. (b) Schulman, J. M.; Venanzi, T. J. *Tetrahedron Lett.* **1976**, 1461. (c) Pomerantz, M.; Fink, R.; Gray, G. A. *J. Am. Chem. Soc.* **1976**, *98*, 291. (d) See also: Horner, M.; Hünig, S. *Ibid.* **1977**, *99*, 6122. (e) Finkelmeier, H.; Lüttke, W. *Ibid.* **1978**, *100*, 6261.
(19) Woodward, R. B.; Hoffmann, R. *Angew. Chem.* **1969**, *81*, 797. *Angew. Chem., Int. Ed. Engl.* **1969**, *8*, 781.
(20) Calculated from the theoretically estimated heat of formation of cyclobutane (−8.1 kcal/mol) minus the experimentally determined heat of formation (6.8 kcal/mol (ref 7b, Table I)).
(21) The calculated (1) and experimentally (2) determined heats of formation follow: (1) 49.6; (2) 51.9 kcal/mol.
(22) Configuration interaction between the ground state and the doubly excited configuration has no effect on energy minima and maxima of the computed electronic hypersurface. This is in agreement with previous recognitions on carbene reactions.[1]

Estimation of Excited-State Redox Potentials by Electron-Transfer Quenching. Application of Electron-Transfer Theory to Excited-State Redox Processes

C. R. Bock, J. A. Connor, A. R. Gutierrez, Thomas J. Meyer,* D. G. Whitten, B. P. Sullivan, and J. K. Nagle

Contribution from the Department of Chemistry, The University of North Carolina, Chapel Hill, North Carolina 27514. *Received July 3, 1978*

Abstract: Rate constants for electron-transfer quenching of $Ru(bpy)_3^{2+*}$ (bpy is 2,2′-bipyridine) by a series of organic quenchers have been determined in acetonitrile (μ = 0.1 M) at 22 ± 2 °C. The reactions studied were based on three different series of structurally related quenchers having varying redox potentials. They include oxidative quenching both by a series of nitroaromatics ($ArNO_2$) and by a series of bipyridinium ions (P^{2+}) and reductive quenching by a series of aromatic amines (R_2NAr). After corrections for diffusional effects, the quenching rate constant (k_q') data fall into two classes both of which can be treated successfully using Marcus–Hush theory. For case I, which includes the data for oxidative quenching by P^{2+} and reductive quenching by R_2NAr, $RT \ln k_q'$ varies as $\Delta G_{23}/2$ where $|\Delta G_{23}| \ll \lambda/2$. ΔG_{23} is the free energy change for electron-transfer quenching within an association complex between the quencher and excited state and λ is the vibrational contribution to the activation barrier to electron transfer. The experimental data are also consistent with Marcus–Hush theory over a more extended range in ΔG_{23} where the free energy dependence includes a quadratic term. For case II, which includes quenching by several of the nitroaromatics, $RT \ln k_q'$ varies as ΔG_{23} and evidence is obtained from the remainder of the data for a transition in behavior from case II to case I. The microscopic distinction between the two cases lies in competitive electron transfer to give either ground- or excited-state products following the electron-transfer quenching step. For case II, back-electron transfer (k_{32}) to give the excited state, e.g., $Ru(bpy)_3^{3+},ArNO_2^- \rightarrow Ru(bpy)_3^{2+*},ArNO_2$, is more rapid than electron transfer to give the ground state (k_{30}), e.g., $Ru(bpy)_3^{3+},ArNO_2^- \rightarrow Ru(bpy)_3^{2+},ArNO_2$. For case I, electron transfer to give the ground state is more rapid. The different behaviors are understandable using electron-transfer theory when account is taken of the fact that k_{30} is a radiationless decay rate constant, and the electron-transfer process involved occurs in the abnormal free-energy region where $-\Delta G_{23} > \lambda$. An appropriate kinetic treatment of the quenching rate data allows estimates to be made of redox potentials for couples involving the excited state. Formal reduction potentials in CH_3CN (μ = 0.1 M) at 22 ± 2 °C are $E(RuB_3^{3+/2+*}) = -0.81 \pm 0.07$ V and $E(RuB_3^{2+*/+}) = +0.77 \pm 0.07$ V. Comparisons between ground- and excited-state potentials show that the oxidizing and reducing properties of the $Ru(bpy)_3^{2+}$ system are enhanced in the excited state by the excited-state energy, that the excited state is unstable with respect to disproportionation into $Ru(bpy)_3^{+}$ and $Ru(bpy)_3^{3+}$, and that the excited state is thermodynamically capable of both oxidizing and reducing water at pH 7. A comparison between the estimated 0–0 energy of the excited state and the energy of emission suggests that there may be only slight differences in vibrational structure between the ground and excited states.

Introduction

Molecular excited states which are sufficiently long lived to be in thermal equilibrium with their surroundings are distinct entities having characteristic chemical and physical properties of their own.[1] An excited-state property which is potentially exploitable in net light to chemical energy conversion processes is the enhanced ability of excited states to function as both oxidants and reductants compared with the ground state.[2,3] Mataga and Weller and their co-workers have shown that electron transfer can be a common reaction for organic excited states[4,5] and more recent work has demonstrated the same reactivity for metal complex excited states, the most notable example being the emitting charge transfer (CT) excited state of $Ru(bpy)_3^{2+}$ (bpy is 2,2′-bipyridine).[2,6]

Perhaps the most fundamental properties associated with electron-transfer reactivity are redox potentials. In earlier communications[7] we reported an experimental approach to the estimation of a reduction potential for the excited-state couple $Ru(bpy)_3^{3+/2+*}$. The approach was based on rate studies for the quenching of $Ru(bpy)_3^{2+*}$ by a series of nitroaromatics having varying strengths as oxidants. The analysis of the data was based on a kinetic scheme used by Rehm and Weller for electron-transfer quenching of fluorescence from a series of aromatic compounds.[5] Since our initial report, additional quenching studies on $Ru(bpy)_3^{2+*}$ and other excited states have given similar results.[8-10]

We have now completed studies of the oxidative quenching of $Ru(bpy)_3^{2+*}$ by a series of dipyridinium ions like paraquat

0002-7863/79/1501-4815$01.00/0

Table I. Rate Constants for the Quenching of $Ru(bpy)_3^{2+*}$ by Aromatic Amines in Acetonitrile (μ = 0.1 M, 22 ± 2 °C)

entry	quencher	$E_{1/2}$, V[a]	k_q, M^{-1} s^{-1} [b]	k_q', M^{-1} s^{-1} [c]
1	p-$Me_2NC_6H_4NMe_2$	0.12 (70, 1.00)[d]	1.2×10^{10}	2.8×10^{10}
2	p-$Me_2NC_6H_4$-$C_6H_4NMe_2$	0.43 (78, 0.98)[d]	4.3×10^9	5.4×10^9
3	p-$Me_2NC_6H_4OMe$	0.55 (71, 0.95)[d]	5.0×10^9	6.5×10^9
4	p-$Me_2NC_6H_4Me$	0.71 (74, 1.02)[d]	1.5×10^9	1.6×10^9
5	10-methylphenothiazine	0.73[e]	1.6×10^9	1.7×10^9
6	$Et_2NC_6H_5$	0.76 ± 0.04[f]	1.5×10^8	1.5×10^8
7	$Me_2NC_6H_5$	0.81 ± 0.05[f]	7.2×10^7	7.2×10^7
8	p-$Me_2NC_6H_4Cl$	0.89 (77, 0.95)[d]	7.4×10^8	7.4×10^8
9	$N(C_6H_5)_3$	1.06 ± 0.03[f]	9.5×10^5	9.5×10^5

[a] As reduction potentials (±0.01 V) for the $D^{+/0}$ couples in CH_3CN (μ = 0.1 M, 22 ± 2 °C) vs. SCE. [b] ±5%. $[Ru(bpy)_3^{2+}] = 3 \times 10^{-5}$ M. k_q was calculated from K_{sv} using $\tau_0(RuB_3^{2+*}) = 850$ ns. [c] Chemically activated rate constants calculated from k_q with corrections made for diffusional effects using eq 3. [d] The values in parentheses are ΔE_p (in mV) and i_c/i_a values, respectively. [e] B. A. Kowert, L. Marcoux, and A. J. Bard, *J. Am. Chem. Soc.*, **94**, 5538 (1972). [f] These couples are electrochemically irreversible. The procedure used for estimating $E_{1/2}$ values is described in the Experimental Section.

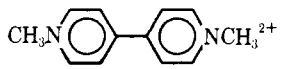

paraquat[11]

in addition to the nitroaromatics and of reductive quenching by a series of aromatic amines like *N,N*-dimethylaniline.[12] The results are of value in demonstrating how quenching rate data can be used to estimate excited-state potentials. The potentials themselves have important implications for the lifetime and electron-transfer properties of the excited state. In addition, an appropriate analysis of the quenching data is instructive in terms of electron-transfer processes which occur both during and after the quenching step. Further, the analysis presented here reveals the existence of competitive electron-transfer processes which give ground- or excited-state products and allows the application of electron-transfer theory to excited-state electron-transfer reactions to be tested over a wide range of ΔG values.

Experimental Section

Materials. Spectroquality acetonitrile (MCB) was used as the solvent for all experiments. Tetraethylammonium perchlorate (Eastman) was recrystallized from ethanol and vacuum dried. The nitroaromatics were obtained commercially and purified as described elsewhere.[11f] The preparation and purification of the dipyridinium salts was also described previously.[11e] *N,N*,4-Trimethylbenzenamine, *N,N*-dimethylbenzenamine, and *N,N*-diethylbenzenamine were purchased from Aldrich and used as received after their purity had been checked by boiling point and ^1H NMR measurements. 4-Methoxy- and 4-chloro-*N,N*-dimethylbenzenamine were prepared from the reaction[13] between the corresponding primary amine and dimethyl sulfate (Eastman), followed by workup according to the method of Sekiya[14] ($4\text{-}MeOC_6H_4NMe_2$, mp 48 °C, bp 125–127 °C (12 Torr); $4\text{-}ClC_6H_4NMe_2$, mp 36 °C, bp 114 °C (12 Torr)). *N,N,N',N'*-Tetramethyl-1,4-benzenediamine (Aldrich) was recrystallized from deoxygenated aqueous ethanol immediatedly prior to use (mp 51 °C). The pure amines were handled under nitrogen. All other reagents were purchased commercially as reagent grade chemicals and used without further purification. $[Ru(bpy)_3]^{2+}$ was used as ClO_4^- or PF_6^- salts which were known to be analytically pure.

Quenching Measurements. Samples for quenching measurements in acetonitrile contained $[Ru(bpy)_3]^{2+}$ ($1\text{-}3 \times 10^{-5}$ M) with the appropriate concentration of added quencher and with enough $[N(C_2H_5)_4](ClO_4)$ added to maintain the ionic strength at 0.1 M. In a typical experiment, solutions containing six different concentrations of quencher were placed in Pyrex tubes closed by rubber serum caps. The solutions were bubble degassed with dry nitrogen for 15–30 min. Emission measurements were made using a Hitachi-Perkin-Elmer MPF-2A spectrofluorimeter.

Flash Photolysis. Flash photolysis experiments were carried out on solutions which had been bubble deaerated with purified nitrogen or in the case of the amine quenchers, freeze–pump–thaw degassed to $\lesssim 10^{-4}$ Torr. The solutions were made up containing $Ru(bpy)_3^{2+}$ (1.0×10^5 M), appropriate amounts of quencher, and sufficient $[N(C_2H_5)_4]ClO_4$ to make μ = 0.1 M. The flash photolysis spectrometers used have been described previously.[11f,15]

Electrochemical Measurements. Cyclic voltammetric measurements on the amine quenchers were performed in CH_3CN solution at a Pt disk working electrode with 0.1 M $[N(n\text{-}C_4H_9)_4](PF_6)$ as supporting electrolyte. The concentration of the amines was kept at $(1.5 \pm 0.3) \times 10^{-3}$ M in all experiments. At higher concentrations of amine, electrode fouling occurred which often resulted in severe distortions in the cyclic voltammetric waves.

As a rule the photochemical experiments were carried out using $[N(C_2H_5)_4](ClO_4)$ as added electrolyte and $[N(n\text{-}C_4H_9)_4](PF_6)$ was used in the electrochemical experiments. Experience has shown that the two salts can be used interchangeably for the two different types of experiments without noticeable differences in the results obtained.

Table I lists $E_{1/2}$ values as reduction potentials, $R_2NAr^+ + e \rightarrow R_2NAr$, vs. the SSCE. It is important to note that the compounds with para-substituted phenyl groups, i.e., p-$Me_2NC_6H_4X$ (X = Cl, Me, $-NMe_2$, $-C_6H_4NMe_2$ and $-OMe$) were all reversible one-electron couples as reported earlier.[16,17] Values for the current ratio of the cathodic to anodic current maxima, i_c/i_a, varied only from 0.95 to 1.02. The peak to peak separation for the forward to reverse scans varied from 71–78 mV independent of scan rate which is similar to the $Ru(bpy)_3^{3+/2+}$ couple itself and probably arises from uncompensated resistance the particular cell–solvent–electrolyte system used in our experiments.

Several of our measured $E_{1/2}$ values are not in good agreement with reported literature values. For instance, Adams reports that for p-$Me_2NC_6H_4Me$, $E_{1/2}$ = 0.65 V in CH_3CN solution with 0.1 M tetraethylammonium perchlorate as supporting electrolyte.[17] Under our conditions $E_{1/2}$ was found reproducibly to be 0.73 V. Likewise, *N,N,N',N'*-tetramethyl(1,1'-biphenyl)-4,4'-diamine is reported to have its first oxidation at $E_{1/2}$ = 0.32 by Mann and Barnes;[16] we find it to be at 0.43 V. The external factors responsible for the variations are not clear.

Because of a lack of suitable reversible couples with appropriate potentials it was necessary to use three irreversible one-electron quenchers, NPh_3, Et_2NPh, and Me_2NPh. Flash photolysis studies show that these $NR_3^{+/0}$ couples are chemically reversibly on the flash photolysis time scale. Following flash photolysis, $Ru(bpy)_3^+$ and NR_3^+ are observed spectroscopically and the solutions are photochromic for several flashes. However, one-electron oxidation of these aryl amines is known to give the transient radical cations which on a longer time scale undergo dimerization.[17] The equation below, due to Olmstead et al.,[18] allows an estimate to be made for the thermodynamic E_0 values for the couples from the initial concentration of the electroactive species (C_0), the second-order rate constant for the dimerization (k_2), the scan rate (v), and the peak potential (E_p),

$$n(E_p - E_0) = (RT/3F)[\ln \psi - 3.12]$$

where

$$\psi = k_2 C_0 RT/nFv$$

The use of the equation is restricted to planar electrodes. In our ex-

Table II. Rate Constants for the Quenching of $Ru(bpy)_3^{2+*}$ by Bipyridinium Ions in Acetonitrile (μ = 0.1 M, 22 ± 2 °C)

entry	quencher	$-E_{1/2}$, V[a]	k_q, M^{-1} s^{-1} [b]	k_q', M^{-1} s^{-1} [c]
1	$[2,7\text{-dimethyldiazaphenanthrene}]^{2+}$	0.42	2.9×10^9	4.0×10^9
2	$[4,4'\text{-}MeNC_5H_4\text{-}C_5H_4NMe]^{2+}$	0.46	2.4×10^9 [d]	3.1×10^9
3	$[trans\text{-}4,4'\text{-}MeNC_5H_4CH{=}CHC_5H_4NMe]^{2+}$	0.50	2.4×10^9	3.1×10^9
4	$[trans\text{-}2,2'\text{-}MeNC_5H_4CH{=}CHC_5H_4NMe]^{2+}$	0.52	1.6×10^9	1.9×10^9
5	$[trans\text{-}2,3'\text{-}MeNC_5H_4CH{=}CHC_5H_4NMe]^{2+}$	0.60	5.6×10^8	5.6×10^8
6	$[trans\text{-}3,4'\text{-}MeNC_5H_4CH{=}CHC_5H_4NMe]^{2+}$	0.63	7.7×10^8 [d]	8.3×10^8
7	$[2,2'\text{-}MeNC_5H_4\text{-}C_5H_4NMe]^{2+}$	0.73	9.1×10^7	9.2×10^7
8	$[3,3'\text{-}MeNC_5H_4\text{-}C_5H_4NMe]^{2+}$	0.84	1.0×10^6	1.0×10^6
9	$[trans\text{-}3,3'\text{-}MeNC_5H_4CH{=}CHC_5H_4NMe]^{2+}$	0.85	1.6×10^6 [d]	1.6×10^6

[a] As reduction potentials (±0.01 V) for the $P^{2+/+}$ couples in CH_3CN (μ = 0.1 M, 22 ± 2 °C) vs. SCE from S. Hunig, J. Gross, and W. Schenk, *Justus Liebigs. Ann. Chem.*, 324 (1973). [b] ±5%. k_q calculated from K_{sv} using $\tau_0(RuB_3^{2+*})$ = 850 ns.[15] [c] Calculated from k_q with corrections made for diffusional effects. [d] Competitive energy transfer is important. The values represent the contribution to k_q from electron-transfer quenching only.[11b,e]

Table III. Rate Constants for the Quenching of $Ru(bpy)_3^{2+*}$ by a Series of Nitroaromatics in CH_3CN (μ = 0.1 M, 22 ± 2 °C)

entry	quencher	$-E_{1/2}$, V[a]	k_q, M^{-1} s^{-1} [b]	k_q', M^{-1} s^{-1} [c]
1	$p\text{-}NO_2C_6H_4NO$	0.52[d]	9.2×10^9	1.6×10^{10}
2	$p\text{-}NO_2C_6H_4NO_2$	0.69[e]	8.6×10^9	9.6×10^9
3	$o\text{-}NO_2C_6H_4NO_2$	0.81[f]	3.1×10^9	3.6×10^9
4	$p\text{-}NO_2C_6H_4CHO$	0.86[e]	2.0×10^9	2.2×10^9
5	$m\text{-}NO_2C_6H_4NO_2$	0.90[e]	1.6×10^9	1.7×10^9
6	$p\text{-}NO_2C_6H_4CO_2CH_3$	0.95[e]	6.6×10^8	6.8×10^8
7	$4,4'\text{-}NO_2C_6H_4\text{-}C_6H_4NO_2$	1.00[g]	1.2×10^8	1.2×10^8
8	$cis\text{-}4,4'\text{-}NO_2C_6H_4CH{=}CHC_6H_4NO_2$	1.00[h]	1.8×10^8	1.8×10^8
9	$m\text{-}NO_2C_6H_4CHO$	1.02[e]	4.9×10^7	4.9×10^7
10	$m\text{-}NO_2C_6H_4COOCH_3$	1.04[e]	1.7×10^7	1.7×10^7
11	$4\text{-}ClC_6H_4NO_2$	1.06[e]	8.0×10^6	8.0×10^6
12	$4\text{-}FC_6H_4NO_2$	1.13[e]	8.3×10^5	8.3×10^5
13	$C_6H_5NO_2$	1.15[e]	2.2×10^5	2.2×10^5

[a] As reduction potentials (±0.01 V) for the $ArNO_2^{0/-}$ couples in CH_3CN vs. SCE (μ = 0.1 M, 22 ± 2 °C). [b] ±5%. $[RuB_3^{2+}] = 10^{-5}$ M. k_q calculated using $\tau_0(RuB_3^{2+*})$ = 850 ns. [c] Calculated from k_q with corrections made for diffusional effects. [d] M. E. Peover, *Trans. Faraday Soc.*, **58**, 2370 (1962). [e] A. H. Maki and D. H. Geske, *J. Am. Chem. Soc.*, **83**, 1852 (1961). [f] A. H. Maki and D. H. Geske, *J. Chem. Phys.*, **33**, 825 (1960). [g] J. E. Harriman and A. H. Maki, *ibid.*, **39**, 778 (1963). [h] G. M. Brown, unpublished result.

periments, a Pt button of known surface area was used and the conditions were such that $|\psi| \leq 10$.

Adams has reported that the dimerization of NPh_3 proceeds with a k_2 value of $\sim 2.4 \times 10^3$.[17] Using this value, the equation above, and E_p values measured at a series of scan rates between 0.02 and 0.5 V/s allowed an average value of E_0 = 1.06 ± 0.03 V to be calculated for the $NPh_3^{+/0}$ couple. In spectroelectrochemical experiments Adams et al.[16b] have reported that the cation Me_2NPh^+ cannot be detected whereas NPh_3^+ is observed before the dimerization step. This indicates that k_2 for Me_2NPh, and probably for Et_2NPh as well, is $>2.4 \times 10^3$. By using k_2 values ranging from 2.4×10^3 to 2.4×10^4 and experimental scan rates between 0.02 and 0.5 V/s, average values of E_0 for the couples $Me_2NPh^{+/0}$ (0.80 ± 0.05V) and $Et_2NPh^{+/0}$ (0.76 ± 0.04) were calculated using the equation above.

Results

The results of the quenching experiments are shown in Table I for the amine quenchers, in Table II for the dipyridinium quenchers and in Table III for the nitroaromatic quenchers. The data were plotted according to the Stern–Volmer equation, $I_0/I = 1 + k_q\tau_0[Q]$ where k_q is the experimental quenching rate constant, τ_0 is the excited-state lifetime for $Ru(bpy)_3^{2+*}$, I_0 is the intensity of light emitted at a fixed wavelength in the absence of quencher, and I is the emitted intensity in solutions with added quencher. The plots were linear over a range of quencher concentrations and the intercepts were unity as expected. k_q values were determined from the slopes of lines using τ_0 = 850 ns for $Ru(bpy)_3^{2+*}$ in acetonitrile (μ = 0.1 M) at 22 ± 2 °C.[11d] The k_q' values cited in the tables are k_q values which have been corrected for diffusional effects using eq 3 below.

Discussion

Reduction potentials for the ground-state $Ru(bpy)_3^{3+/2+}$ (1.29 V) and $Ru(bpy)_3^{2+/+}$ (−1.33 V) couples are known from electrochemical measurements in acetonitrile (μ = 0.1 M) vs. the SCE.[19] In the reduced form of the $Ru(bpy)_3^{2+/+}$ couple, an electron is added to a ligand-based π^*(bpy) level rather than to a metal-based level.[12a,19]

Low-temperature emission and transient absorption measurements show that in the excited state, $Ru(bpy)_3^{2+*}$, there are orbitally well-defined oxidation (Ru(III)) and reduction ($(bpy^{-\cdot})_3$) sites based on the metal and ligands, respectively.[20] The excited state is relatively long lived in solution (850 ns in CH_3CN at 22 ± 2 °C). It is sufficiently long lived to be in thermal equilibrium with its surroundings and should have its own distinctive thermodynamic properties including oxidation ($Ru(bpy)_3^{2+*} \rightarrow Ru(bpy)_3^{3+} + e$) and reduction ($Ru(bpy)_3^{2+*} + e \rightarrow Ru(bpy)_3^{+}$) potentials. When written as reduction potentials, values for the excited- and ground-state couples are related as shown in eq 1a where ΔG_{ES} is the excess free-energy content of the excited state over the ground state. Given the ground-state potentials, numerical values for the two excited-state couples in acetonitrile are related as shown in eq 1b.

$$\Delta G_{ES}(V) = E(RuB_3^{3+/2+}) - E(RuB_3^{3+/2+*}) = E(RuB_3^{2+*/+}) - E(RuB_3^{2+/+}) \quad (1a)$$

(B = 2,2′-bipyridine)

$$E(RuB_3^{3+/2+*}) = -E(RuB_3^{2+*/+}) - 0.04 \quad (1b)$$

The major theme of this paper is the estimation of excited-state redox potentials for $Ru(bpy)_3^{2+*}$ using the oxidative quenching data in Tables II and III for the $Ru(bpy)_3^{3+/2+*}$ couple and the reductive quenching data in Table I for the

$Ru(bpy)_3^{2+*/+}$ couple. The procedure to be followed will be (1) the development of a kinetic analysis for the quenching reactions, (2) application of electron-transfer theory to the quenching step, and (3) use of the theoretically predicted dependence of the quenching rate constants on ΔG to estimate excited-state potentials.

Before beginning the analysis it is important to establish that the quenching reactions do occur by electron transfer since energy transfer is, at least in principle, a competing process. Electron- and energy-transfer quenching are known to be competitive processes in the quenching of $Ru(bpy)_3^{2+*}$ by certain of the bipyridinium ions like $[trans\text{-}MeNC_5H_4CH{=}CHC_5H_4NMe]^{2+}$ ($E_T \sim 50$ kcal/mol), and the k_q' values in Table II have been corrected for a contribution from energy transfer.[11b,c] For ions like $[MeNC_5H_4\text{-}C_5H_4NMe]^{2+}$, the triplet energies are too high[21] for energy transfer to be competitive with electron transfer. For the amine quenchers, triplet energies again appear to be too high (68.9 kcal mol^{-1} for Me_2NPh) for energy transfer to compete with reductive quenching.[22]

For both the bipyridinium ions and amines like $Me_2NC_6H_5$, the expected redox products are observed following flash photolysis (e.g., $Ru(bpy)_3^+$ and $Me_2NC_6H_5^+$).[11,12] We have also observed that $Ru(bpy)_3^{2+*}$ is quenched by a series of amines like $p\text{-}NO_2C_6H_4NMe_2$ ($E_T = 54$ kcal/mol)[23] which have electron-withdrawing substituents on the aromatic ring.[24] However, the absence of redox products following flash photolysis suggests that the mechanism of quenching may be energy transfer and the results obtained will be discussed in a different context in a later paper.

For the nitroaromatics, the situation is less clear. Separated redox products are not observed following flash photolysis but that might be expected given the attractive charge types produced by oxidative quenching, $Ru(bpy)_3^{3+}$,$ArNO_2^-$.[11f,25] As discussed below, the ion separation step to give the ions $Ru(bpy)_3^{3+} + ArNO_2^-$ is in competition with back-electron transfer to $Ru(bpy)_3^{3+}$. The ion separation step is expected to be slower in the nitroaromatic quenching reactions because of the electrostatic attraction between the quenching products.

Additional strong evidence for predominant electron-transfer quenching in all three cases comes from the variation of the k_q' values with ΔG as discussed in the next section.

Analysis of the Quenching Rate Data. A kinetic scheme for excited-state quenching by electron transfer is shown in eq 2 using as an example reductive quenching of $Ru(bpy)_3^{2+*}$ by an aromatic amine (D). The scheme is based on an earlier one given by Rehm and Weller for the fluorescence quenching of a series of aromatic excited states.[5] In eq 2, k_{12} and k_{21} are

$$\begin{array}{ccccc} RuB_3^{2+*} + D & \overset{h\nu}{\underset{1/\tau_0}{\rightleftharpoons}} & RuB_3^{2+} + D & & \\ k_{12} \downarrow\uparrow k_{21} & & & & \\ RuB_3^{2+*},D & \underset{k_{32}}{\overset{k_{23}}{\rightleftharpoons}} & RuB_3^{+},D^+ & \xrightarrow{k_{30}} & \begin{cases} \xrightarrow{k_1} RuB_3^+ + D^+ \\ \xrightarrow{k_2} RuB_3^{2+},D \end{cases} \end{array} \quad (2)$$

forward and reverse rate constants for the formation of an association complex between the excited state and D prior to electron transfer. The equilibrium constant for formation of the complex is $K_{12} = k_{12}/k_{21}$. k_{23} is the rate constant for electron-transfer quenching of the excited state within the association complex. k_{32} is the rate constant for the corresponding back-electron-transfer reaction to return to the excited state. k_{30} is a combined rate constant for processes following the quenching step which lead to net quenching rather than to repopulation of the excited state. The processes include back-electron transfer to give ground-state $Ru(bpy)_3^{2+}$ (k_2) rather than the excited-state $Ru(bpy)_3^{2+*}$ and a competitive step where the redox products, $D^+ + Ru(bpy)_3^+$, separate in solution (k_1).

Before interpreting the quenching data in terms of eq 2, it is necessary to make corrections for diffusional effects using eq 3. This is necessary because, for the most rapid of the quenching reactions, the rate constants approach the diffusion-controlled limit.[26] In eq 3, k_q is the measured quenching rate constant, k_q' is the rate constant for activated quenching, and k_D is the diffusion-limited rate constant in the medium of interest. The k_q' values in Tables I–III were calculated using $k_D = 2.1 \times 10^{10}$ M^{-1} s^{-1} for the neutral amine and nitroaromatic quenchers and $k_D = 1.0 \times 10^{10}$ M^{-1} s^{-1} for the dipyridinium quenchers.[27]

$$1/k_q = 1/k_q' + 1/k_D \quad (3)$$

A kinetic analysis of the scheme in eq 2 gives eq 4a where $F = k_{30}/(k_{30} + k_{32})$ is the fraction of electron-transfer quenching events which lead to net quenching. By using the expression $k_{23} = \nu_{23} \exp(-\Delta G^*_{23}/RT)$ for the electron-transfer quenching step, eq 4a becomes eq 4b. Δ_{23} and ΔG^*_{23} are the free energy of activation and frequency factor for the electron-transfer quenching step (k_{23}).

$$k_q' = k_{23}K_{12}F = k_{23}K_{12}[k_{30}/(k_{30} + k_{32})] \quad (4a)$$

$$k_q' = K_{12}F\nu_{23} \exp(-\Delta G^*_{23}/RT) \quad (4b)$$

From the theoretical work of Marcus and Hush, the free energy of activation for the quenching step is given[30,31] by

$$\Delta G^*_{23} = \lambda/4[1 + (\Delta G_{23}/\lambda)]^2 \quad (5)$$

ΔG_{23} is the free-energy change which occurs on electron-transfer quenching within the association complex and $\lambda/4$ is the contribution to the activation barrier for electron transfer which arises from the need to reorganize the inner (λ_i) and outer (λ_o) coordination spheres prior to electron transfer. ΔG_{23} can be calculated from reduction potential values for the redox couples involved if the electrostatic energies associated with bringing together the reactants (W_r; $D + Ru(bpy)_3^{2+*}$) and products (W_p; $D^+ + Ru(bpy)_3^+$) are taken into account:

$$\text{reduction: } \Delta G_{23}(V) = -[E(RuB_3^{2+*/+}) - E(Ox/Red)] + W_p - W_r \quad (6a)$$

$$\text{oxidation: } \Delta G_{23}(V) = -[E(Ox/Red) - E(RuB_3^{3+/2+*})] + W_p - W_r \quad (6b)$$

Equation 6a applies to reductive quenching and 6b to oxidative quenching. $E(Ox/Red)$ stands for reduction potential values for the $ArNO_2^{0/-}$, $P^{2+/+}$, or $R_2NAr^{+/0}$ couples. The electrostatic energies can be calculated for acetonitrile at 22 °C using eq 7 in which z_A and z_B are the ion charges, μ is the ionic strength, and d is the distance (in Å) beween the ion centers.

$$W(\text{kcal/mol}) = (9.10Z_AZ_B/d)[1/(1 + 0.48d\sqrt{\mu})] \quad (7)$$

Combining the theoretically derived dependence of ΔG^*_{23} on ΔG_{23} in eq 5 with eq 4b gives

$$k_q' = K_{12}F\nu_{23} \exp\left[-\lambda/4\left(1 + \frac{\Delta G_{23}}{\lambda}\right)^2/RT\right] \quad (8)$$

Equation 8 is an important step in the right direction since it contains an explicit relationship between ΔG_{23} and the quenching rate constants. If the rate data could be used to evaluate ΔG_{23} for a particular reaction, the excited-state potentials would be accessible using eq 6a or 6b since reduction potentials for the individual quenchers are known from electrochemical measurements.

There are two limiting forms for the expressions for k_q' given in eq 4 and 8. They depend on the relative magnitudes of the rate constants which make up the fraction, F. In case I, net

quenching by ion separation and back-electron transfer to give ground-state $Ru(bpy)_3^{2+}$; e.g., $Ru(bpy)_3^+, D^+ \rightarrow Ru(bpy)_3^{2+}$, D, is more rapid than back-electron transfer to give the excited-state, $Ru(bpy)_3^+, D^+ \rightarrow Ru(bpy)_3^{2+*}$, D. Under these conditions and referring back to eq 2, $k_{30} \gg k_{32}$ and $F = 1$. Equations 4 and 8 then give

$$k_q' = k_{23}K_{12} = K_{12}\nu_{23}\exp\left[-\lambda/4\left(1 + \frac{\Delta G_{23}}{\lambda}\right)^2/RT\right] \quad (9)$$

In case II, back-electron transfer to give the excited state becomes the rapid process, $k_{32} \gg k_{30}$ and $F = k_{30}/k_{32}$, and eq 4 and 8 become

$$k_q' = k_{23}K_{12}(k_{30}/k_{32}) = k_{30}K_{12}K_{23} = k_{30}K_{12}\exp(-\Delta G_{23}/RT) \quad (10)$$

In the intermediate region where $k_{30} \sim k_{32}$, k_q' is given by

$$k_q' = \frac{\nu_{23}k_{30}K_{12}}{k_{30}\exp(\Delta G^*_{23}/RT) + \nu_{23}\exp(\Delta G_{23}/RT)} \quad (11)$$

For our purposes, the most useful equations are eq 9 and 10 in logarithmic form,

$$\text{case I: } RT\ln k_q' = \left(RT\ln \nu_{23}K_{12} - \frac{\lambda}{4}\right) - \frac{\Delta G_{23}}{2}\left(1 + \frac{\Delta G_{23}}{2\lambda}\right) = RT\ln k_q'(0) - \frac{\Delta G_{23}}{2}\left(1 + \frac{\Delta G_{23}}{2\lambda}\right) \quad (12)$$

$$\text{case II: } RT\ln k_q' = RT\ln k_{30}K_{12} - \Delta G_{23} \quad (13)$$

In eq 12 it is assumed that, since we are dealing with a series of structurally and electronically related quenchers and the same excited state, the product, $\nu_{23}K_{12}$, and the reorganizational barrier, $\lambda/4$, should be reasonably constant throughout the series. The $k_q'(0)$ values are then characteristic constants for each series of quenchers. They can be interpreted as chemically activated electron-transfer rate constants for a hypothetical quencher where $\Delta G_{23} = 0$.

For those quenchers where ΔG_{23} is small, either + or −, a simpler form of eq 12 can be used since if $|\Delta G_{23}| \ll 2\lambda$, the term $\Delta G_{23}/2\lambda$ in eq 12 is negligible which gives

$$\text{case I: } RT\ln k_q' = RT\ln k_q'(0) - (\Delta G_{23}/2) \quad (14)$$

It is convenient to express eq 12 and 14 in terms of the experimentally determined reduction potentials for the quencher couples, $E(Ox/Red)$. It follows from eq 6, which relates ΔG_{23} and $E(Ox/Red)$, that:

case I

reduction: $RT\ln k_q' = RT\ln k_q'(0) - \frac{E(Ox/Red)}{2} + \frac{1}{2}[E(RuB_3^{2+*/+}) + W_p - W_r]$ (15a)

oxidation: $RT\ln k_q' = RT\ln k_q'(0) + \frac{E(Ox/Red)}{2} - \frac{1}{2}[E(RuB_3^{3+/2+*}) + W_p - W_r]$ (15b)

case II

reduction: $RT\ln k_q' = RT\ln k_{30}K_{12} - E(Ox/Red) + [E(RuB_3^{2+*/+}) + W_p - W_r]$ (16a)

oxidation: $RT\ln k_q' = RT\ln k_{30}K_{12} + E(Ox/Red) - [E(RuB_3^{3+/2+*}) + W_p - W_r]$ (16b)

Our procedure for estimating excited-state potentials now follows directly from eq 15 and 16. First for eq 15 and case I behavior, the following obtains. If a plot of $RT\ln k_q'$ vs. $E(Ox/Red)$ for a related series of quenchers has a linear region of slope = ½, the theoretically predicted free-energy dependence in eq 15 will have been established. Now we define a potential, $E(0)(Ox/Red)$, for the hypothetical quencher couple for which $\Delta G_{23} = 0$. $E(0)(Ox/Red)$ can be determined from the plot of $RT\ln k_q'$ vs. $E(Ox/Red)$ if an independent estimate for $k_q'(0)$ can be made. It follows from eq 14 that $E(0)$-(Ox/Red) is the quencher potential for which $RT\ln k_q'$ (on the plot) = $RT\ln k_q'$ (calcd). Once $E(0)(Ox/Red)$ is known, the potential for the excited-state couple can be calculated. It follows from eq 6a that, for reductive quenching,

$$E(RuB_3^{2+*/+}) = E(0)(Ox/Red) - (W_p - W_r) \quad (17a)$$

and from eq 6b that, for oxidative quenching,

$$E(RuB_3^{3+/2+*}) = E(0)(Ox/Red) - (W_p - W_r) \quad (17b)$$

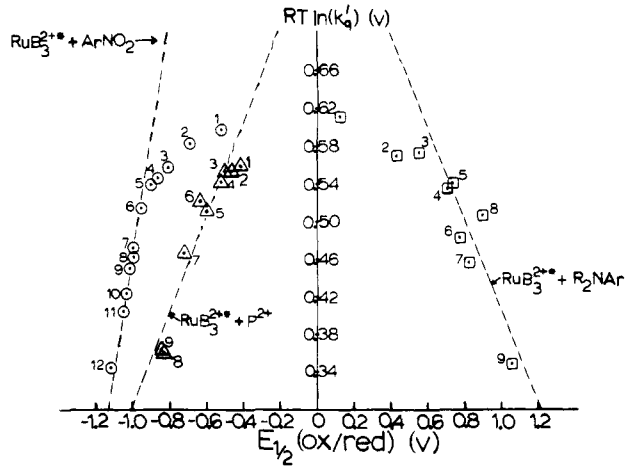

Figure 1. Plot of $RT\ln k_q'$(V) vs. $E_{1/2}$(Ox/Red)(V) in CH_3CN (μ = 0.1 M) at 22 ± 2 °C for the quenching of $Ru(bpy)_3^{2+*}$ by R_2NAr (□), P^{2+} (△), and $ArNO_2$ (○). Data were taken from Tables I–III. Lines of slope = ½ are shown drawn through the experimental data for the R_2NAr and P^{2+} points and a line of slope = 1 through the $ArNO_2$ data.

In Figure 1 are shown plots of $RT\ln k_q'$ vs. $E(Ox/Red)$ for the three sets of quenching reactions. Dashed lines of slope = ½ are drawn through the data points for oxidative quenching by the bipyridinium ions, P^{2+}, and for reductive quenching by the amines, R_2NAr. A line of slope = 1 is drawn through the nitroaromatic, $ArNO_2$, quenching data.

For the P^{2+} and R_2NAr quenchers the predictions of eq 15 are borne out for a reasonable span in $E(Ox/Red)$ values. As discussed in a later section, where curvature appears in the plots, ΔG_{23} is no longer small compared with 2λ and the quadratic form of eq 12 fits the data reasonably well. The procedure will now be to estimate $k_q'(0)$ independently so that a numerical value for $E(0)(Ox/Red)$ can be determined.

For the nitroaromatics, the slope = 1 behavior of eq 16a holds over a range in $E(Ox/Red)$ values. The origin of the curvature is first a transition from case II to case I behavior followed by a transition to the quadratic form of eq 12, but this will also be discussed in a later section. To calculate the excited-state potential from eq 17b, $k_{30}K_{12}$ must be estimated and $E(0)(Ox/Red)$ determined from the linear part of the plot where $RT\ln k_q' = RT\ln k_{30}K_{12}$.

Assuming that self-exchange rate constants remain essentially the same for a series of related quenchers, $\ln k_q'(0)$ can be calculated from

$$\ln k_q'(0) = \frac{1}{2}\ln k_{11}k_{22} + (W_{11} + W_{22} - 2W_r)/2RT \quad (18)$$

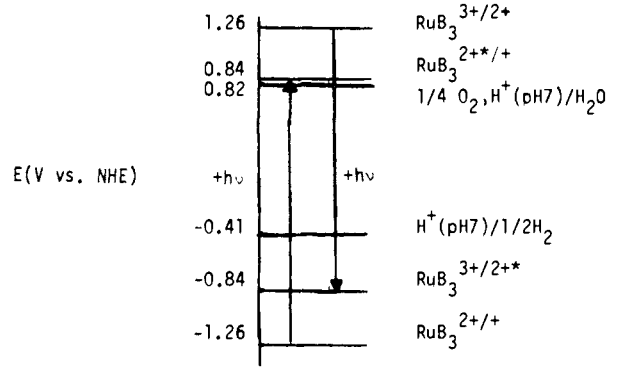

Figure 2. Redox potential diagram.

Equation 18 is derived from the Marcus "cross-reaction" equation,[31] $k_q' = (k_{11}k_{22}K_{23})^{1/2}$, where $K_{23} = 1 (\Delta G_{23} = 0)$. k_{11} and k_{22} are the self-exchange rate constants for the quencher and excited-state couples, W_{11}, W_{22}, and W_r are the electrostatic energies or work terms for bringing together the reactants for the two self-exchange reactions and for the quenching reaction, respectively. The added term, $(W_{11} + W_{22} - 2W_r)/2RT$, in eq 18 is necessary because of the differences in charge types between the self-exchange and quenching reactions.[32]

It is possible to use eq 18 to calculate $\ln k_q'(0)$ for the amine quenchers, but self-exchange rate data for the $P^{2+/+}$ couples have apparently not been reported. Self-exchange rate constants of $(1.0 \pm 0.2) \times 10^9$ M^{-1} s^{-1} and $(7.5 \pm 0.8) \times 10^8$ M^{-1} s^{-1} have been measured for the couples $[p\text{-}Me_2NC_6H_4C_6H_4NMe_2]^{+/0}$ and $[p\text{-}Me_2NC_6H_4C_6H_4NH_2]^{+/0}$ in CH_3CN at 25 °C (μ = 0.1 M).[33] An estimate for the $Ru(bpy)_3^{2+*/+}$ self-exchange reaction of $k = 5 \times 10^8$ M^{-1} s^{-1} (25 °C, μ = 0.5 M) has been made by Toma and Creutz.[8] Using the latter estimate but corrected to a value appropriate in CH_3CN at μ = 0.1 M (4×10^8 M^{-1} s^{-1}),[34,35] an average value of 8.7×10^8 M^{-1} s^{-1} for the amine couples and eq 18 gives, for the hypothetical quenching reaction where $\Delta G_{23} = 0$, $k_q'(0) = 8.8 \times 10^8$ M^{-1} s^{-1} or $RT \ln k_q'(0) = 0.52$ V. From the line of slope = ½ drawn through the amine quenching data in Figure 1, the potential $E(0)(R_2NAr^{+/0})$ at which $RT \ln k_q' = RT \ln k_q'(0) = 0.52$ V occurs at 0.76 V. Using this value for $E(0)[R_2NAr^{+/0}]$, the potential for the excited state acting as an oxidant can be calculated from eq 17a ($W_r = 0$, $W_p \approx 0.01$ V).[27] If an uncertainty of ±10 is assumed in the estimate for $k_q'(0)$, $E(RuB_3^{2+*/+}) = 0.77 \pm 0.10$ V and from eq 1b, which relates the potentials for the excited state acting as oxidant and reductant, $E(RuB_3^{3+/2+*}) = -0.81 \pm 0.10$ V.

Redox potentials for the excited-state couples can also be estimated using the data for oxidative quenching of $Ru(bpy)_3^{2+*}$ by the nitroaromatic quenchers. From the plot in Figure 1, the data for points 6–12 follow what was described as case II behavior in that a plot of $RT \ln k_q'$ vs. ΔG_{23} is linear with slope = 1. Now it is necessary to make an independent estimate of the product $k_{30}K_{12}$. If $k_{30}K_{12}$ were known, an extrapolation of the plot of $RT \ln k_q'$ vs. $E(ArNO_2^{0/-})$ to the potential where $RT \ln k_q' = RT \ln k_{30}K_{12}$ would give $E(0)(ArNO_2^{0/-})$. This limiting situation is strictly a hypothetical case since, with the real quenchers, the transition between case II to case I behavior has already occurred as ΔG_{23} becomes less positive and reaches 0 (Figure 1).

A reasonable estimate is that $k_{30}K_{12} = 4 \times 10^{11}$ s^{-1}.[37] Using that value and $RT \ln k_q'(0) = RT \ln k_{30}K_{12} = 0.68$ V, it follows from the plot in Figure 1 that $E(0)(ArNO_2^{0/-}) = -0.77$ V. From eq 17b, $E(RuB_3^{3+/2+*}) = -0.81$ V ($W_r = 0$; $W_p = -0.04$ V). Assuming that the uncertainty in the product $k_{30}K_{12}$ is ±10 gives $E(RuB_3^{3+/2+*}) = -0.81 \pm 0.07$ V.

Table IV. Formal Reduction Potentials at Room Temperature (μ = 0.1 M)

couple	E, V (CH_3CN vs. SCE)	E, V (H_2O vs. NHE)[a]
$Ru(bpy)_3^{3+/2+}$	1.29 ± 0.07	1.26
$Ru(bpy)_3^{2+*/+}$	0.77 ± 0.07	0.84
$Ru(bpy)_3^{3+/2+*}$	−0.81 ± 0.07	−0.84
$Ru(bpy)_3^{2+/+}$	−1.33 ± 0.07	−1.26

[a] Reference 41.

The approach used here to estimate excited-state potentials appears to be reasonable. There are theoretical bases for the two different kinetic analyses used and the agreement between them is satisfying. The precision of the estimates is restricted on one hand by the availability of self-exchange rate data and the scatter in experimental points and on the other by the value chosen for $k_{30}K_{12}$.

Our approach based on excited-state quenching may provide a general procedure for the estimation of excited-state potentials, but obvious limitations exist. They include cases where energy transfer is competitive with electron transfer, where there are insufficient data in the critical ΔG_{23} region, and where the data do not conform to one of the two limiting cases.

Redox Potentials and Their Implications for Excited-State Properties. The results of the quenching experiments provide internally consistent estimates of the potentials for the two excited-state couples $Ru(bpy)_3^{2+*/+}$ and $Ru(bpy)_3^{3+/2+*}$. The uncertainties in the values seem unavoidable given the nature of the experiments and the approximations used, although the kinetic treatment appears to be adequate. Hopefully, the approach outlined here will provide a basis for at least crude estimates of potentials for additional excited-state redox couples in the future.

Potentials for the ground- and excited-state couples involving $Ru(bpy)_3^{2+}$ are summarized in Table IV. The data are given as formal reduction potentials both in water and in acetonitrile.

Several interesting features about the potentials have been noted in previous papers[2,3,42] including the fact that the excited state is thermodynamically capable of both oxidizing and reducing water at pH 7. The redox potential data are summarized below using both a Latimer-type diagram

$$Ru(bpy)_3^{3+} \xrightarrow{-0.81} Ru(bpy)_3^{3+*} \xrightarrow{+0.78} Ru(bpy)_3^{+}$$

$$\uparrow \Delta G_{ES}$$

$$Ru(bpy)_3^{3+} \xrightarrow{1.29} Ru(bpy)_3^{2+} \xrightarrow{-1.33} Ru(bpy)_3^{+}$$

volts vs. SCE in CH_3CN, μ = 0.1 M

and a redox potential diagram (Figure 2). From the potential diagrams, the oxidizing and reducing powers of $Ru(bpy)_3^{2+}$ are enhanced in the excited state by ΔG_{ES} where ΔG_{ES} is the free-energy content of the excited state above the ground state. The enhanced oxidizing and reducing properties of the excited state mean that it is unstable with respect to disproportionation into $Ru(bpy)_3^{3+}$ and $Ru(bpy)_3^{+}$ and a recent experiment has shown that the disproportionation reaction can be catalyzed chemically.[42]

From the difference in the ground- and excited-state potentials in Table IV, ΔG_{ES} for $Ru(bpy)_3^{2+*}$ is 2.10 V. Spectroscopic studies on the excited state show that there is a slight contribution to ΔG_{ES} from an entropic difference of electronic origin ($T\Delta S \sim 0.03$ V),[43] but the major contribution is apparently enthalpic and the 0–0 energy of the excited state can

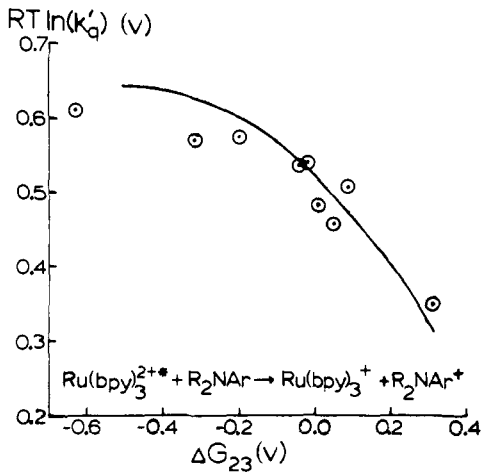

Figure 3. Plot of $RT \ln k_q'$ vs. ΔG_{23} in CH_3CN (μ = 0.1 M) at 22 ± 2 °C for the quenching of $Ru(bpy)_3^{2+*}$ by R_2NAr. The theoretical line was drawn using eq 12, $k_q'(0) = 8.8 \times 10^8\ M^{-1}\ s^{-1}$, and λ = 11 kcal/mol (0.48 V).

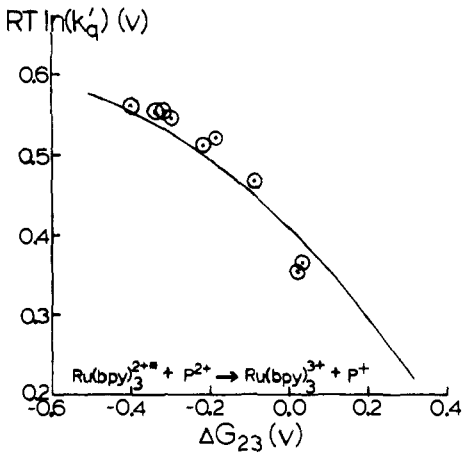

Figure 4. Plot of $RT \ln k_q'$ vs. ΔG_{23} in CH_3CN (μ = 0.1 M) at 22 ± 2 °C for the quenching of $Ru(bpy)_3^{2+*}$ by P^{2+}. The points were calculated using eq 12, $k_q'(0) = 8.4 \times 10^6$ from Figure 1, and λ = 17 kcal/mol (0.74 V).

be estimated to be E_0 = 2.13 V. λ_{max} for emission from $Ru(bpy)_3^{2+*}$ in CH_3CN (μ = 0.1 M) is 608 nm giving E_{em} = 2.04 V. The small difference between E_0 and E_{em} reinforces the interpretation given in Crosby's work that absorption (λ_{max} 453 nm) and emission involve different CT states.[20a] The difference in the CT states is that different sets of delocalized π^*(bpy) acceptor levels are involved, $\pi^*(e)$ in absorption and $\pi^*(a_2)$ in emission. The small difference between E_0 and E_{em} also suggests that there may be only slight differences in vibrational structure between the ground and excited states. The absence of major distortions in the excited state would mean that the potential energy surfaces for the two states are not greatly displaced relative to each other which would in turn have important consequences both for the lifetime and electron-transfer reactivity of the excited state.

Competitive Electron Transfer to Give Ground- or Excited-State $Ru(bpy)_3^{2+}$. Implications for Chemiluminescence and Electrochemiluminescence Yields. In discussing the results of their fluorescence quenching experiments, Rehm and Weller noted that the free energy dependence predicted by Marcus-Hush for the electron-transfer step (eq 5) did not fit their data in either the normal, $-\Delta G_{23} < \lambda$, or abnormal, $-\Delta G_{23} > \lambda$, free-energy regions.[5] For reactions in the abnormal free-energy region, eq 9 predicts that as ΔG_{23} becomes increasingly favorable k_q' should decrease. Experimentally, Rehm and Weller found that k_q' approached the diffusion-controlled limit with increasing $-\Delta G_{23}$ and no decrease was observed over a wide range in $-\Delta G_{23}$ values. Their results showed that k_q' remained rapid in the abnormal free-energy region and suggested that, in contrast to the strong dependence of k_q' on ΔG_{23} predicted by eq 9, k_q' is, in fact, relatively independent of ΔG_{23}.[44] The failure of the Marcus-Hush prediction in the abnormal free-energy region arises because of its classical origin.[45] Electron transfer in this region is a radiationless decay process involving a transition between different electronic states and the reactant vibrational manifold is within the product manifold. The available experimental evidence[5,45d,46] shows that the absence of a strong dependence on ΔG exists because transition probabilities from equilibrium or near-equilibrium vibrational levels of the reactants are high which is not unexpected quantum mechanically.[45]

Of more immediate interest here is the fact that Rehm and Weller found that equations like 5 and 9 did not fit their data even in the normal free-energy region, and they proposed the empirical equation

$$\Delta G^*_{23} = \frac{\Delta G_{23}}{2} + \sqrt{(\Delta G_{23}/2)^2 + \lambda/4}$$

which did. However, we find that our quenching data and probably the quenching results obtained by Rehm and Weller in the normal free-energy region can be accounted for by the Marcus-Hush theory if events which occur past the quenching step are taken into account.

Consider first the quenching data for the amine and bipyridinium quenchers which are shown plotted as $RT \ln k_q'$ vs. quencher reduction potential in Figure 1. The plots show the slope = ½ behavior predicted for small $|\Delta G_{23}|$ values by eq 14 and 15. Equations 14 and 15 apply to case I behavior where, after electron-transfer quenching has occurred, there is no complication from back-electron transfer to give the excited state. For these quenchers, essentially every electron-transfer quenching event leads to net quenching.

Over a more extended range in ΔG_{23} values, the variation of $RT \ln k_q'$ with ΔG_{23} should take on the quadratic form given by eq 12. In Figures 3 and 4 are shown plots of $RT \ln k_q'$ vs. ΔG_{23} for the two sets of quenchers. The ΔG_{23} values were calculated for each quencher using eq 6, the potentials of the quencher couples, and the potentials of the excited-state couples determined in this work. For the amine quenchers in Figure 3, a theoretical line is shown which was calculated from eq 12 using the experimental estimate of $k_q'(0) = 8.8 \times 10^8\ M^{-1}\ s^{-1}$ mentioned earlier and λ = 11 kcal/mol.[47] For the bipyridinium quenchers, self-exchange rate data are not available but a value of $k_q'(0) = 8.4 \times 10^6\ M^{-1}\ s^{-1}$ can be estimated from the data in Figure 1.[48] The calculated line in Figure 4 is drawn using that value for $k_q'(0)$ and $\lambda \approx 17$ kcal/mol.[47] The agreement between theory and experiment for both sets of quenchers is at least suggestive that the quadratic dependence predicted by Marcus-Hush theory (eq 12) does apply to the excited-state quenching reactions.

For the nitroaromatic quenchers, Figure 5 shows that the situation is more complicated. There is a region where the slope = ½ changing to quadratic dependence found for the other two sets of quenchers does occur. For these quenchers, every electron-transfer quenching event leads to net quenching and the free-energy dependence of the quenching rate constant is predicted by Marcus-Hush theory.

There is also a well-defined region where the slope = 1 behavior predicted by eq 13 and 16 for case II occurs. For these quenchers, electron-transfer quenching is unfavorable (ΔG_{23} > 0.2 V). However, once quenching has occurred, back-electron transfer to give the excited state (k_{32} in eq 19) is favored

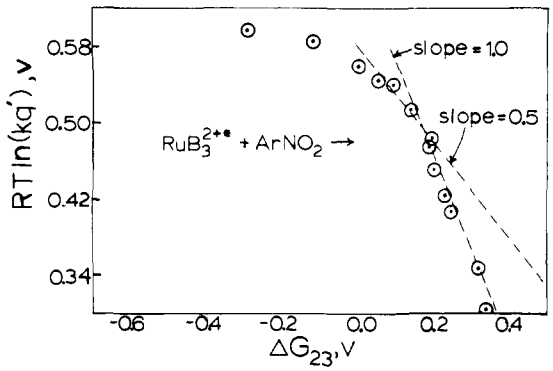

Figure 5. Plot of $RT \ln k_q'$ vs. ΔG_{23} (μ = 0.1 M) at 22 ± 2 °C for the quenching of $Ru(bpy)_3^{2+*}$ by $ArNO_2$.

($\Delta G_{32} < -0.2$ V) since $\Delta G_{32} = -\Delta G_{23}$. From the kinetic treatment which led to case II behavior, the rate constant for net quenching is now slower than back-electron transfer to give the excited state ($k_{30} \ll k_{32}$). Under these conditions, the quenching step is a rapid preequilibrium which is followed by rate-determining ion separation or back-electron transfer to give ground-state $Ru(bpy)_3^{2+}$. For the nitroaromatics, flash photolysis studies show that ion separation is relatively unimportant so that net quenching occurs dominantly by electron transfer to give the ground state (k_{30} in eq 19).

$$RuB_3^{2+*},ArNO_2 \underset{k_{32}(\Delta G_{32})}{\overset{k_{23}(\Delta G_{23})}{\rightleftharpoons}} RuB_3^{3+},ArNO_2^- \xrightarrow[(\Delta G_{30})]{k_{30}} RuB_3^{2+},ArNO_2 \quad (19)$$

It is now possible to discuss the transition between the slope = 1 (case II) and slope = ½ (case I) behaviors in terms of the two reactions which compete after the quenching step. Although both are electron-transfer reactions, they are fundamentally different kinds of processes. The k_{32} step, which is the reverse of quenching, is an excited-state interconversion process. Note Figure 6. The difference between the two states is the position of the excited electron. It is in π^*(bpy) in $[Ru(bpy)_3^{2+*},ArNO_2]$ and in $\pi^*(ArNO_2)$ in $[Ru(bpy)_3^{3+},ArNO_2^-]$, and, in this sense, the quenched-state $[Ru(bpy)_3^{3+},ArNO_2^-]$ is an outer-sphere analogue of the $Ru(bpy)_3^{2+}$ MLCT excited state itself. Although the k_{32} step involves a conversion between excited states, it is an electron-transfer reaction in the normal free-energy region since ΔG_{32} is in the range of −0.4 to +0.4 V (Figure 5) and $-\Delta G_{32} < \lambda$ (note below). If the k_{32} step is a normal electron transfer reaction, it follows from eq 9 that the dependence of k_{32} on ΔG_{32} or ΔG_{23} should be given by

$$k_{32} = \nu_{32} \exp(-\Delta G^*_{32}/RT)$$
$$= \nu_{32} \exp\left[-\frac{\lambda}{4}\left(1 + \frac{\Delta G_{32}}{\lambda}\right)^2 \Big/ RT\right]$$
$$= \nu_{32} \exp\left[-\left(1 - \frac{\Delta G_{23}}{\lambda}\right)^2 \Big/ RT\right] \quad (20)$$

The k_{30} step is an electron-transfer reaction which could also be described as radiationless decay of an excited state to the ground state. It is formally similar and, in fact, is the outer-sphere analogue of radiationless decay of the MLCT excited state of $Ru(bpy)_3^{2+}$ (k_{rd} in Figure 6). The free-energy change for the reaction, ΔG_{30}, is given by

$$\Delta G_{30} \simeq -(\Delta G_{23} + \Delta G_{ES}) = \Delta G_{32} - \Delta G_{ES} \quad (21)$$

where ΔG_{ES} is the free-energy content of the excited state above the ground state. Values of ΔG_{30} calculated using eq 21

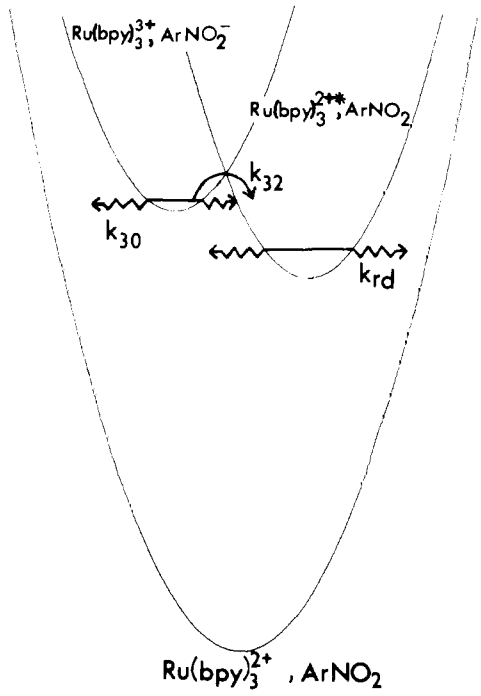

Figure 6. Reaction coordinate diagram for competitive electron transfer to give either ground- or excited-state $Ru(bpy)_3^{2+}$ following oxidative quenching by a nitroaromatic ($ArNO_2$).

fall in the range of −1.7 to −2.5 V. The values of ΔG_{30} are sufficiently negative that, as electron-transfer reactions, the processes involved fall in the abnormal free-energy region where transitions between different electronic states occur. From the discussion at the beginning of this section, which concerned the free-energy dependence of reactions in this region, it follows that k_{30} should be relatively independent of ΔG_{30} and ΔG_{32} and k_{30} should therefore be essentially constant for the series of quenchers.

It is the difference in free-energy dependence between k_{30} and k_{32} that can be used to explain the transition between case II and case I behavior in Figure 5. Although k_{30} is constant at a value near $k_{30} \geq 5 \times 10^{10}$ s^{-1},[37] k_{32} will vary with ΔG_{32} as in eq 20. Only for those quenchers where the free-energy change on quenching is unfavorable ($\Delta G_{23} > 0.2$ V) will ΔG_{32} be appreciably favorable. These are the only cases where, following the quenching step, electron transfer to give excited-state $Ru(bpy)_3^{2+}$ is sufficiently favorable to compete with electron transfer to give the ground state.

In fact, the point is best illustrated by some sample calculations. Self-exchange rate constants for the $ArNO_2^{0/-}$ couples fall in the range 10^8–10^9 M^{-1} s^{-1}.[33] If it is assumed that λ = 13 kcal/mol,[47] that $\Delta G_{32} = -0.2$ V, and that $\nu_{32} = 10^{13}$ s^{-1},[49] the rate constant for electron transfer to give the excited state is calculated to be $k_{32} = 10^{12}$ s^{-1} using eq 20. This value is significantly larger than the estimate $k_{30} \geq 5 \times 10^{10}$ s^{-1} for electron transfer to give the ground state. The relative magnitudes of the two constants are consistent with the assumption that $k_{30} \ll k_{32}$ which was used in the derivation of slope = 1 behavior for case II. For quenchers where ΔG_{32} is less favorable, k_{32} will decrease and, as ΔG_{32} becomes less favorable, k_{32} will fall below k_{30} leading to the transition between case II and case I behavior. As an example, assuming that ΔG_{32} = 0, $\nu_{32} = 10^{13}$ s^{-1}, and λ = 13 kcal/mol, $k_{32} = 4 \times 10^{10}$ s^{-1} is obtained which is near the value $k_{30} \geq 5 \times 10^{10}$ s^{-1} estimated in ref 37.

The results obtained here may be of relevance in understanding the magnitude of emission yields obtained in chemi-

luminescence and electrochemiluminescence (ecl) experiments. For example, in an ecl experiment where $ArNO_2^-$ and $Ru(bpy)_3^{3+}$ are generated electrochemically, the kinetic scheme involved would be essentially the reverse of eq 2:

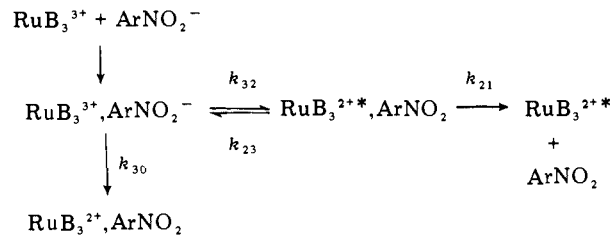

Only for those cases where ΔG_{32} is sufficiently negative so that k_{32} is at least comparable with k_{30} will luminescence be observed, a prediction which is verifiable experimentally.

Acknowledgments are given to the National Science Foundation under Grants CHE77-03423 and CHE14405 for support of this work and to Professor Vincenzo Balzani for preprints of his work.[6a,10] J.A.C. thanks the W. R. Kenan, Jr., Foundation and the U.K. Science Research Council for a Visiting Professorship and a Senior Visiting Fellowship at The University of North Carolina, Chapel Hill, respectively. Further, he thanks the University of Manchester for leave of absence and the Council for the International Exchange of Scholars for a Fulbright-Hays Senior Award.

References and Notes

(1) A. W. Adamson in "Concepts of Inorganic Photochemistry", A. W. Adamson and P. D. Fleischauer, Ed., Wiley-Interscience, New York, 1975, Chapter 10.
(2) (a) T. J. Meyer, *Acc. Chem. Res.*, **11**, 94 (1978); (b) T. J. Meyer in "Fundamental Research in Homogeneous Catalysis", M. Tsutsui and R. Ugo, Eds., Plenum Press, New York, 1977, p 169; (c) N. Sutin, *J. Photochem.*, **10**, 19 (1979).
(3) C. Creutz and N. Sutin, *Proc. Natl. Acad. Sci. U.S.A.*, **72**, 2858 (1975).
(4) N. Mataga and N. Nakashima, *Spectrosc. Lett.*, **8**, 275 (1975).
(5) D. Rehm and A. Weller, *Ber. Bunsenges. Phys. Chem.*, **73**, 834 (1969); *Isr. J. Chem.*, **8**, 259 (1970).
(6) (a) V. Balzani, F. Bolletta, M. T. Gandolfi, and M. Maestri, *Top. Curr. Chem.*, **75**, 1 (1978); (b) T. J. Meyer, *Isr. J. Chem.*, **15**, 200 (1977).
(7) C. R. Bock, D. G. Whitten, and T. J. Meyer, *J. Am. Chem. Soc.*, **97**, 2909 (1975); C. R. Bock, J. A. Connor, A. R. Gutierrez, T. J. Meyer, B. P. Sullivan, and J. K. Nagle, *Chem. Phys. Lett.*, in press.
(8) H. E. Toma and C. Creutz, *Inorg. Chem.*, **16**, 545 (1977).
(9) R. Scheerer and M. Gratzel, *J. Am. Chem. Soc.*, **99**, 865 (1977).
(10) R. Ballardini, G. Varani, M. T. Indelli, F. Scandola, and V. Balzani, *J. Am. Chem. Soc.*, **100**, 7219 (1978).
(11) (a) C. R. Bock, D. G. Whitten, and T. J. Meyer, *J. Am. Chem. Soc.*, **96**, 4710 (1974); (b) A. R. Gutierrez, T. J. Meyer, and D. G. Whitten, *Mol. Photochem.*, 7, 349 (1976); (c) R. C. Young, D. G. Whitten, and T. J. Meyer, *J. Am. Chem. Soc.*, **97**, 4781 (1975); (d) R. C. Young, D. G. Whitten, and T. J. Meyer, *ibid.*, **98**, 286 (1976); (e) A. R. Gutierrez, Ph.D. Dissertation, The University of North Carolina, 1975; (f) C. R. Bock, Ph.D. Dissertation, The University of North Carolina, 1974.
(12) (a) C. P. Anderson, D. J. Salmon, R. C. Young, and T. J. Meyer, *J. Am. Chem. Soc.*, **99**, 1980 (1977); (b) M. Maestri and M. Gratzel, *Ber. Bunsenges. Phys. Chem.*, **81**, 504 (1977).
(13) S. Hünig, *Chem. Ber.*, **85**, 1056 (1952).
(14) M. Sekiya, M. Tomie, and N. J. Leonard, *J. Org. Chem.*, **33**, 318 (1968).
(15) R. C. Young, Ph.D. Dissertation, The University of North Carolina, 1976.
(16) (a) C. K. Mann and K. K. Barnes, "Electrochemical Reactions in Nonaqueous Systems", Marcel Dekker, New York, 1970; (b) E. T. Seo, R. F. Nelson, J. M. Fritsch, L. S. Marcoux, D. W. Leedy, and R. N. Adams, *J. Am. Chem. Soc.*, **88**, 3498 (1966).
(17) R. N. Adams, "Electrochemistry at Solid Electrodes", Marcel Dekker, New York, 1969, p 355.
(18) M. L. Olmstead, R. G. Hamilton, and R. S. Nicholson, *Anal. Chem.*, **41**, 261 (1969).
(19) (a) N. E. Tokel-Takvoryan, R. E. Hemingway, and A. J. Bard, *J. Am. Chem. Soc.*, **95**, 6582 (1973); (b) T. Saji and S. Aoyagui, *J. Electroanal. Chem. Interfac. Electrochem.*, **58**, 401 (1975); (c) D. J. Salmon, Ph.D. Dissertation, The University of North Carolina, 1976.
(20) (a) K. W. Hipps and G. A. Crosby, *J. Am. Chem. Soc.*, **97**, 7042 (1975), and references therein; (b) J. Van Houten and R. J. Watts, *ibid.*, **98**, 4853 (1976); (c) R. Benasson, C. Salet, and V. Balzani, *ibid.*, **98**, 3722 (1976).
(21) A. Ledwith, *Acc. Chem. Res.*, **5**, 133 (1972).
(22) (a) C. Dubroca and P. Lozano, *Chem. Phys. Lett.*, **24**, 49 (1974); E. C. Lin and S. K. Chakrabati, *ibid.*, **24**, 49 (1974); (b) J. N. Demas and G. A. Crosby, *J. Am. Chem. Soc.*, **93**, 2841 (1971).
(23) R. Foster, D. L. Hammick, G. M. Hood, and A. C. E. Sander, *J. Chem. Soc.*, 5865 (1956).
(24) J. A. Connor, unpublished results.
(25) R. C. Jarnagin, *Acc. Chem. Res.*, **4**, 420 (1971).
(26) R. M. Noyes, *Prog. React. Kinet.*, **1**, 129 (1961).
(27) For the calculations here and those described later, $r = 7.1$ Å was used for $Ru(bpy)_3^{2+*}$, $Ru(bpy)_3^{2+}$, and $Ru(bpy)_3^{3+}$ and an average van der Waals radius of 3.8 Å was used for the various quenchers. The average values were estimated by taking the average of the van der Waals dimensions along three molecular axes. k_O for the neutral quenchers was calculated using the Smoluchowski equation[28]
$$k_O = (2RT/3000\eta)(2 + r_A/r_B + r_B/r_A)$$
where the Stokes–Einstein equation has been used to calculate diffusion coefficients for the reactants of radii r_A and r_B in a medium of viscosity η. The Debye–Smoluchouski equation[29]
$$k_O = (2RT/3000\eta)(2 + r_A/r_B + r_B/r_A)f$$
was used to calculate k_D for the dipyridinium quenchers where f is the integral $[a\int_a^\infty (e^{u/kT})dr/r^2]^{-1}$ and $u = (Z_A Z_B e^2/D_s)[e^{\kappa a}/(1 + \kappa a)](e^{-\kappa r}/r)$ where the various terms are r = distance of separation of ions; a = distance of closest approach of ions = $r_A + r_B$; D_s = static dielectric constant of the pure solvent; Z_A, Z_B = charges on ions; e = unit electron charge; $\kappa = [(8N_0e^2\mu/1000D_skT)]^{1/2}$; N_0 = Avogadro's number. The integral was evaluated numerically using Simpson's rule. For the quenching of $Ru(bpy)_3^{2+}$ by the pyridinium ions in 0.1 M CH_3CN, $f = 0.50$ and $k_D = 1.01 \times 10^{10}$ M^{-1} s^{-1}.
(28) M. von Smoluchowski, *Z. Phys. Chem.*, **92**, 129 (1917).
(29) P. Debye, *Trans. Electrochem. Soc.*, **82**, 265 (1942).
(30) (a) N. S. Hush, *Trans. Faraday Soc.*, **57**, 557 (1961). (b) N. S. Hush, *Prog. Inorg. Chem.*, **8**, 391 (1967); *Electrochim. Acta*, **13**, 1005 (1968); *Chem. Phys.*, **10**, 361 (1975).
(31) R. A. Marcus, *J. Chem. Phys.*, **24**, 966 (1956); **43**, 679 (1965). R. A. Marcus and N. Sutin, *Inorg. Chem.*, **14**, 213 (1975), and references therein.
(32) A. Haim and N. Sutin, *Inorg. Chem.*, **15**, 476 (1976).
(33) B. A. Kowert, L. Marcoux, and A. J. Bard, *J. Am. Chem. Soc.*, **94**, 5538 (1972).
(34) A correction for the difference in W_r between the two media was made using eq 7.
(35) For λ_O, the equation[2a,30,31,36]
$$\lambda_O = e^2(1/2r_A + 1/2r_B - 1/d)(1/n^2 - 1/D_s)$$
was used where r_A and r_B are the molecular radii of the reactants (7.1 Å), d is the internuclear separation in the activated complex for electron transfer, and n^2 (= 1.81) and D_s (= 37.5) are the optical and static dielectric constants of the solvent which is acetonitrile.
(36) R. C. Young, F. R. Keene, and T. J. Meyer, *J. Am. Chem. Soc.*, **99**, 2468 (1977).
(37) The assumption that $k_{30}K_{12} = 4 \times 10^{11}$ s^{-1} is not unreasonable. From their data on the fluorescence quenching of aromatic excited states, Rehm and Weller estimate that $k_{30}K_{12} \geq 8 \times 10^{10}$.[5] As calculated from the Fuoss–Eigen equation,[38-40]
$$K = (2.524 \times 10^{-3})d^3 \exp(-W_r/RT)$$
$K_{12} = 3.3$ for the nitroaromatic quenching reactions ($W_r = 0$; $d = 10.9$ Å), which is a factor of ~4 greater than for their cases. It is also possible to make an indirect estimate for k_{30} from the quenching points 1–5 in Figure 1. These points fall in the transition region between cases I and II, and for the first few points $k_{30} > k_{32}$ as discussed in a later section. Since no redox products are observed following flash photolysis, from eq 3, $k_{30} = k_1 + k_2 \sim k_2$. k_1 can be estimated from $K = k_1/k_{-1}$ for the equilibrium
$$RuB_3^{3+},ArNO_2^- \underset{k_{-1}}{\overset{k_1}{\rightleftharpoons}} RuB_3^{3+} + ArNO_2^-$$
From the Fuoss equation $K = 0.062$ (acetonitrile, $d = 10.9$ Å, $\mu = 0.1$, $Z_A = 3$, $Z_B = -1$), $k_O = 4.2 \times 10^{10}$ (see ref 27), and $k_1 = 2.6 \times 10^9$ s^{-1}. Given the sensitivity of the flash photolysis apparatus used,[15] k_2 must exceed k_1 by ≥ 20 so that $k_{30} = k_2 \geq 5 \times 10^{10}$ s^{-1}. With this value of k_{30}, $k_{30}K_{12} \geq 1.5 \times 10^{11}$.
(38) R. M. Fuoss, *J. Am. Chem. Soc.*, **94**, 75 (1972).
(39) P. Hemmes, *J. Am. Chem. Soc.*, **94**, 75 (1972).
(40) C. T. Lin and D. B. Rorabacher, *Inorg. Chem.*, **12**, 2402 (1973).
(41) C. Creutz and N. Sutin, *Inorg. Chem.*, **15**, 496 (1976).
(42) J. K. Nagle, R. C. Young, and T. J. Meyer, *Inorg. Chem.*, **16**, 3366 (1977).
(43) From their low temperature spectroscopic studies, Crosby and co-workers have concluded that for the excited state there is a manifold of four low-lying levels A_1, E, and A_2 with the E and A_2 states lying 10 and 61.2 cm^{-1} above A_1.[20a] Because of the small energy spacings, essentially all four of the levels are occupied at room temperature leading to an effective increase in multiplicity in the excited state. There are also a series of higher levels, but they are relatively far removed from the lowest manifold of levels.
(44) Actually, once the diffusion-controlled limit is approached, experimental information about k_q' is lost. k_q' could in fact increase with increasing $-\Delta G_{23}$, but it certainly does not decrease at least to any significant extent.
(45) (a) R. P. Van Duyne and S. F. Fischer, *Chem. Phys.*, **5**, 183 (1974); (b) S. Efrima and M. Bixon, *Chem. Phys. Lett.*, **25**, 34 (1974); (c) W. Schmickler, *J. Chem. Soc., Faraday Trans.*, **72**, 307 (1976); (d) J. K. Nagle, W. D. Dressick, and T. J. Meyer, *J. Am. Chem. Soc.*, in press.
(46) C. Creutz and N. Sutin, *J. Am. Chem. Soc.*, **99**, 241 (1977).
(47) λ values were estimated using the Marcus equation, $k = Z\exp(-\lambda/4RT)$,[31] using the self-exchange constants for k and assuming that $Z = 10^{11}$ s^{-1}.
(48) The estimate was made using eq 14 and the data in Figure 1. Using

$E(RuB_3^{3+/2+*}) = -0.81$ V, $W_p - W_r = 0.01$ V, and eq 17 gives $E(0)(P^{2+/+})$ $= -0.82$ V. Since $E(0)(P^{2+/+})$ is the quencher potential where $\Delta G_{23} = 0$, at that potential on the plot in Figure 1, $RT \ln k_q' = RT \ln k_q'(0) = 0.41$ V.

(49) (a) M. J. Powers, D. J. Salmon, R. W. Callahan, and T. J. Meyer, *J. Am. Chem. Soc.*, **98**, 6731 (1976); (b) J. C. Curtis and T. J. Meyer, *Ibid.*, **100**, 6284 (1978); (c) B. P. Sullivan and T. J. Meyer, submitted for publication.

Application of Force Field Calculations to Organic Chemistry. 8.[1] Internal Rotation in Simple to Congested Hydrocarbons Including 2,3-Dimethylbutane, 1,1,2,2-Tetra-*tert*-butylethane, 2,2,4,4,5,5,7,7-Octamethyloctane, and Cholestane

Eiji Ōsawa,* Haruhisa Shirahama, and Takeshi Matsumoto

Contribution from the Department of Chemistry, Faculty of Science, Hokkaido University, Sapporo 060, Japan. *Received November 6, 1978*

Abstract: Allinger's new force field MM2 was tested for the calculation of barrier heights of internal rotation about the C–C bond in simple to congested acyclic hydrocarbons. This force field performs satisfactorily for simple hydrocarbons but systematically underestimates barrier heights for highly congested molecules. MM2 calculations were performed to investigate beyond experimental limits novel features of internal rotation in several molecules of current interest. Conformers having nonalternating Newman projections proposed recently by Mislow are confirmed to appear in the torsional itinerary of 2,3-dimethylbutane. 1,1,2,2-Tetra-*tert*-butylethane (**1**) is predicted to possess a distorted gauche ground-state conformation of $(FB)_3$, or essentially FBE_2, rotamer type. Between this global energy minimum and gauche–anti barrier is a wide torsional range in which the novel F_2BFB_2 rotamer type dominates. Internal compression effects were postulated in order to explain the unusually high rotational barrier of the central C–C bond of 2,2,4,4,5,5,7,7-octamethyloctane (**2**) and these were analyzed in some detail and given strong support. In addition, skeletal twisting and unique valence angle variations accompanying the internal rotation of **2** are also attributed to the compression effects. Steric energies of rotamers of cholestane (**3**) regarding the rotation about the C_{17}–C_{20} bond have been calculated to clarify the controversy over their relative stabilities. They are separated by low barriers (at most 12 kcal/mol). Rotational barriers about the bond between C_{17} and various alkyl substituents are calculated for models of **3**, and the reason for the reported failure of freezing C_{17}–*tert*-butyl bond rotation is rationalized.

One of the most useful applications of empirical force field calculations[2] to organic chemistry is the analysis of dynamic molecular processes such as the pseudorotations of ring compounds[3] and the correlated rotations of bulky substituents.[4,5] The internal rotation about C–C bonds in alkanes[6] has, however, been treated by this theoretical method only sporadically.[7-12] Recent introduction of truncated Fourier series consisting of one- to threefold cosine functions as an improved expression for torsional potential for saturated molecules,[13,14] instead of the familiar $k(1 - \cos 3\omega)$ type,[2] prompted us to perform systematic survey calculations on the ability of the force field to reproduce experimental barrier heights of C_{sp^3}–C_{sp^3} bond rotation in acyclic hydrocarbons.[15,16] A few reliable barrier values have recently been obtained for simple to congested alkanes by the dynamic NMR method.[18]

The improved torsional potential has been incorporated into two new force fields: Bartell's MUB-2[19] and Allinger's MM2.[20] The latter was used throughout this work.[21]

As described below, the MM2 force field performed well for simple hydrocarbons but was revealed to underestimate rotational barriers for congested molecules. However, the errors appear systematic and the correct barrier heights can be reasonably estimated based on the MM2-calculated barriers. On the basis of these results, we studied several current topics of internal rotation in some detail. They include the appearance of nonalternating rotamers during internal rotation, the possibility of internal rotations in the extremely crowded 1,1,2,2-tetra-*tert*-butylethane (**1**), the secondary effects of the high rotational barrier of 2,2,4,4,5,5,7,7-octamethyloctane (**2**),

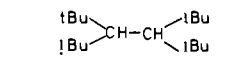

1

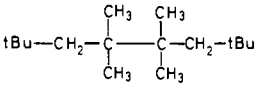

2

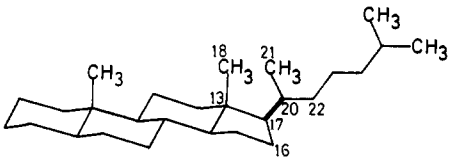

3

and the controversy over the restricted rotation about the C_{17}–C_{20} bond in steroid systems like cholestane (**3**).

Results and Discussion

Comparison between Calculated and Experimental Barriers. *n*-Butane. The torsional itinerary for the rotation about the central bond of *n*-butane was calculated by application of the Wiberg–Boyd bond drive technique.[22] Table I compares the characteristic features of the internal rotation obtained by MM2 with those obtained by partly geometry-optimized 4-31G ab initio molecular orbital calculations[23] and available experimental values. The MM2 anti → gauche barrier is in

0002-7863/79/1501-4824$01.00/0